



Published in final edited form as:

J Orthop Res. 2013 March ; 31(3): 441–447. doi:10.1002/jor.22246.

Predicting Three-dimensional Patellofemoral Kinematics from Static Imaging-Based Alignment Measures

Benjamin R. Freedman and **Frances T. Sheehan, Ph.D.**

Functional and Applied Biomechanics, Department of Rehabilitation Medicine, NIH, Bethesda, MD, USA

Abstract

Patellofemoral pain syndrome causes significant discomfort and disability among much of the general population. Despite recent breakthroughs in dynamic three-dimensional imaging technologies to assess pathological patellofemoral motion, such tools remain costly for clinical diagnostics applications. Thus, this study investigated whether three-dimensional patellofemoral kinematics could be predicted from routine two-dimensional static measures of patellofemoral joint alignment quantified from magnetic resonance imaging (MRI) data acquired in full knee extension. Twenty-six volunteers clinically diagnosed with patellofemoral pain (19F/7M, 25.9±11.1 years) and twenty-six control subjects (19F/7M, 25.3±7.7 years) were included in this IRB-approved study. Static three-dimensional sagittal T1-weighted gradient recall echo and dynamic MRI scans were acquired. For the dynamic image acquisition, subjects cyclically flexed and extended their knee (at 30 cycles/minute) while a full cine-phase contrast MRI set (24 times frames of anatomic images and x, y, and z-velocity images) was acquired. From these data, static measures of patellofemoral alignment and three-dimensional patellofemoral kinematics were derived. Single and multiple regressions between static and kinematic variables were evaluated. Although shown reliable, the static MRI measures could only partially predict patellofemoral kinematics, with r^2 -values ranging from 16%-77%. This makes it imperative that the current precise, accurate, 3D, dynamic imaging techniques be translated into clinical tools.

INTRODUCTION

Patellofemoral pain syndrome (PFPS), defined as long-term idiopathic anterior knee pain, affects approximately 14-17% of the young active population¹. It is theorized to be caused by a force imbalance at the knee² and/or abnormal bone shape^{3,4} that results in pathological patellofemoral (PF) kinematics (pathomechanics)^{5,6}. It is believed that such pathomechanics ultimately lead to increased PF joint stress and pain^{7,8}. Although PFPS is typically exacerbated by dynamic activities requiring active quadriceps loading, clinical evaluation of the knee relies primarily on 2D static imaging-based alignment measures and other clinical markers, because *in vivo* 3D dynamic PF kinematic measures, quantified during activities requiring active muscle control, are not yet clinically available.

Imaging technologies have continuously evolved in order to more accurately and quantitatively evaluate the PF joint (as well as other joints) under loaded dynamic conditions. The first imaging studies evaluating PF alignment^{9,10} were limited to 2D static imaging of the anterior aspect of the PF joint. The required flexed knee posture of roentgenographic imaging resulted in high false negative rates^{9,11}. In the late 1980s, computed tomography (CT) and magnetic resonance imaging (MRI) became available to study PF alignment in a fully-extended position¹²⁻¹⁴. These technologies confirmed that the femoral influence on the patella is lessened as the knee enters terminal extension¹¹, making malalignment most evident in this range¹⁵. Thus, for interventional decisions, particularly invasive ones, CT and MRI are often favored over x-ray^{11,16,17}. Later, cine-MRI was used to quantify 2D PF kinematics during volitional leg extension exercises⁶. The ability to image the PF joint during an activity requiring muscle control⁷ allowed PF pathomechanics to be diagnosed that would have otherwise “been overlooked with static examination techniques”⁶. Advances in imaging technologies have enabled the 3D PF kinematics contractions to be quantified during either dynamic exercise requiring quadriceps activity^{18,19} or statically with active quadriceps²⁰. These 3D studies added to previous findings by documenting kinematic differences beyond the classic axial-plane measures. For example, the results from the Sheehan et al.¹⁸ study supported the long standing association between patella alta and PFPS²¹⁻²³, as well as introduced other kinematic variables that may be key components in the development of PFPS, such as pathological PF valgus and flexion¹⁹. A recent 3D study²⁴ demonstrated that PF flexion (measured during active extension) could discriminate with 100% accuracy the presence of idiopathic long-term anterior knee pain in a cohort of individuals diagnosed with cerebral palsy.

Many of these novel dynamic imaging methodologies have remained research tools, leaving the simpler static 2D imaging-based measures as the primary methods for diagnosing PF joint pathology^{9,10,25}; even though PF pain is typically experienced during dynamic events requiring high quadriceps loading. The validity of predicting 3D PF kinematics from static, 2D, imaging-based measures remains unestablished. Quantifying the relationship between the static and dynamic states of the PF joint may offer improved diagnostics and eventual treatment of suspected patellar maltracking²⁶. Thus, the purpose of this study was to determine if 3D PF kinematics, acquired *in vivo* during a volitional leg extension exercise, could be predicted from 2D, static, image-based measures of PF alignment. A secondary aim was to evaluate the reliability of these static measures.

METHODS

For this retrospective, IRB-approved study two cohorts were established from an existing database (controls [n=90] and subjects diagnosed with PFPS [n=54]). Each subject signed informed consent at the time of enrollment. To be included within the PFPS cohort the subject had to be diagnosed with idiopathic anterior knee pain (> 6 months duration), have no history of lower limb surgery, and have positive clinical signs of patellar maltracking⁵. Subjects included within the control cohort had no current or past history of lower leg pain, injury, surgery, or pathology. All included subjects had a previously acquired dynamic cine phase contrast (CPC) MRI dataset and a 3D static sagittal-plane MRI acquisition with the knee in full extension. Static full extension was defined using visual inspection of the

clinical knee angle (created by lines connecting the hip, knee, and ankle joint centers in the sagittal plane). As a check on this visual alignment, the knee was only considered to be in static full extension if the knee angle, as measured in the sagittal GRE images (Fig 1: the 2D acute angle between t_y and f_y), was within two standard deviations a previous control cohort. For this previous cohort, subjects were placed in full extension, using the same visual alignment procedure, prior to acquiring a sagittal plane 3D GRE image of the knee. If both knees qualified for the study, a single knee was randomly selected (control) or the more impaired knee (PFPS cohort) was selected for inclusion. The final study cohort consisted of 26 controls (19F/7M, 25.3±7.7 years, 166.1±9.3cm, 61.1±11.6kg) and 26 subjects diagnosed with PFPS (19F/7M, 25.9±11.1 years, 165.4±9.1cm, 62.2±10.6kg).

Subjects lay supine in an MRI scanner (1.5 T; GE Medical Systems, Milwaukee, WI; or 3.0 T; Philips Electronics, Eindhoven, The Netherlands) during static and dynamic image acquisition. For static scanning, the knee and hip were fully extended with the mid-patella at the center of a knee coil. The ankle was held in the anatomical neutral position using cushion blocks. Subjects were instructed to keep their muscles relaxed while static 3D sagittal T1-weighted high resolution (1mm³) gradient recall echo (GRE) images were acquired (TR=11, TE=5.1, 70-84 slices, Flip Angle = 15°). Image acquisition ranged from just distal to the tibial tuberosity to just superior to the quadriceps' tendon insertion into the rectus femoris (RF). During dynamic scanning (Fig 1) the subject's knee was placed over a cushioned wedge, slightly flexing the hip and knee. Coupled-phased array coils were supported medial and lateral to the knee using a custom-built coil holder. Subjects cyclically flexed and extended their knee (30 cycles/minute, to the beat of an auditory metronome) while a full CPC image set (anatomic and x-, y-, and z-velocity images over 24 times frames) was acquired in a single sagittal plane. The CPC scanning parameters varied slightly between the 3.0T²⁷ and 1.5T²⁸ scanners, but the overall temporal resolution (61.2 msec on the 3T and 73.6msec on the 1.5T) was kept similar. Although the images were acquired in a single plane, the 3D velocity enabled tracking of musculoskeletal points of interest in all three dimensions. A 3-plane axial cine image set (anatomical images only, 24 time frames) was acquired in order to establish anatomic coordinate systems²⁸.

Seven static measures of interest (Fig 2: patellar tilt angle (PTA), lateral patellar displacement (LPD), anterior/posterior displacement (AP_S), inferior/superior displacement (SI_S), bisect offset (BO), patellophyseal index (PPI), and the RF-Q-angle) were quantified from the 3D GRE images. The subscript "S" denotes static. To quantify these measures, the 3D sagittal GRE images were reconstructed into axial images. Femoral vectors and points of interest were located in axial image at the level of the femoral epicondyle. Likewise, patellar vectors and points of interest were located in mid-patellar axial image. The PTA was quantified as the acute angle between the vectors defining the patellar posterior-lateral border and the femoral posterior edge (Fig 2C). Next, the lateral, anterior, and superior distance from the patellar origin (Po, the most posterior patellar point) to the femoral origin (Fo, the deepest point in the femoral sulcus) was defined as the LPD, AP_S, and SI_S displacement (Fig 2C,F). For the purpose of this study medial, anterior, and superior were considered positive directions. The BO⁶ and the PPI²² were also measured (Fig 2B, E). Lastly, the RF-Q-angle was quantified as the acute angle between two vectors defined by three points (the tibial tuberosity, the anterior-mid-patellar, and the center of RF just

superior to the myo-tendinous junction, Fig 2C,D,F). This measure was created previously to be a more precise measure of the clinical Q-angle. The 2D PF alignment measures were redefined relative to the static femoral coordinate system (Fig 2). This effectively rotated all images such that the posterior edge of the femoral condyles (at the level of the epicondylar width) and the vector bisecting the femoral shaft (in the sagittal plane) were aligned with the image right-left and inferior-superior directions, respectively. This was done to reduce errors from slight variations in subject alignment relative to the magnet²⁵. To account for size variations across subjects, LPD, AP_S, and SI_S were scaled by the ratio of the average epicondylar width from a previous control cohort, 76.9 mm²⁸, to the subject-specific epicondylar width.

PF translation (ML_K, AP_K, SI_K) and rotation (tilt, flexion, and varus rotation) during active extension, was analytically tracked through integration of the CPC data (Fig 1). The accuracy of tracking skeletal kinematics using CPC data is less than 0.5 mm^{27,29} (average absolute error). These six kinematic variables were expressed relative to the dynamic femoral anatomical coordinate system (Fig 1)²⁸, which was defined similar to its static counterpart. PF orientation (Fig 1) was calculated using a body-fixed xyz-Cardan rotation sequence (flexion, tilt, and varus)³⁰. All translations were scaled in an identical manner to the static measures.

Multiple regression analyses were used to establish predictive models for the PF kinematics. To determine which static variables were appropriate as input to the multiple regression analyses, individual linear regressions between each static and each dynamic variable were evaluated. This was followed by a multiple regression analysis (Enter method, SPSS Inc, Chicago, IL, v19), if multiple static variables demonstrated significant linear regressions to a single dynamic variable. The multiple regression model used only those variables. Based on guidelines for correlations³¹, a model with an r^2 value of greater than 0.60 was defined as being strongly predictive. The numerous regression models were susceptible to type I error. Therefore, regressions were reported only if they remained significant after their p-values were adjusted using a Bonferroni-type false discovery rate procedure³². Although the PF kinematics were determined over a large range of motion, the regressions were focused on the PF kinematics from two knee angles (10°, matching the static position, and 20°), both of which could capture the more unstable PF kinematics near full extension. An *a priori* power analysis determined that 26 subjects per cohort were required to determine significant regression between the RF-Q-angle and ML_K ($\alpha=0.05$ and $\beta=0.80$), based on a previous study⁵. Intraclass correlation coefficients (ICCs), using a two-way mixed effects model, were computed to evaluate intra- and inter-rater repeatability of the static PF alignment measures across 25 knees (randomly selected from both cohorts). The two raters were blinded to each others measures, as well as their original measures. A p-value < 0.05 was considered as significant.

RESULTS

The majority of 3D PF kinematics could be predicted from static MRI measures, but static lateral patellar tilt best predicted its dynamic counterpart (r^2 -value ranged from 0.59 to 0.69, Fig 3 and Table 2). Multiple regression analyses tended to increase the r^2 -values (Table 3).

This was particularly true for SI_K in the PFPS cohort, where r^2 increased from 0.38 to 0.77 by adding LPD and RF-Q-angle into the regression. LPD alone could explain 47% ($p < 0.001$) of the variability (PFPS cohort) in ML_K (dynamic lateral shift). This improved to 62% ($p < 0.001$) upon advancing to a multiple regression analysis using both LPD and RF-Q-angle. Varus rotation (PFPS and control cohorts) along with ML_K and AP_K (control cohort) could not be predicted by a single or multiple static variables.

The regressions at 20° were typically weaker than at 10° and, thus were not reported. This leads to the likely conclusion that the predictive values worsen with increasing variance between the static and dynamic knee angles.

All static MRI measures showed excellent intra- and inter-rater repeatability, with ICCs ranging from 0.95-0.99 (Table 1). The two cohorts were, on average, very well matched with no significant differences in demographics found between cohorts. The MR based knee angle ($10.6^\circ \pm 3.3^\circ$ and $10.8^\circ \pm 4.2^\circ$ in the control and PFPS cohorts, respectively) tended to overestimate the clinical knee angle.

DISCUSSION

Recent breakthroughs in 3D dynamic imaging technologies^{19,29} have enabled the evaluation of more subtle cases of maltracking⁶ and the testing of numerous underlying assumptions governing modern PFPS diagnostics and interventions^{19;28}. As these 3D dynamic imaging technologies have not been clinically available, an often unstated assumption has been that static imaging can be used as a surrogate for quantifying the dynamic state of the joint under active quadriceps control. The current findings demonstrate that static measures of PF alignment, quantified in 2D images acquired with the knee in full extension, can only predict a portion of the 3D PF kinematics during a loaded volitional task.

Although significant linear regressions existed for most kinematic variables, the majority of their variability could not be explained by a single static surrogate. This low predictability is likely due to the fact that the forces on the patella from femoral sulcus begin to lessen as the knee moves into terminal extension. This allows the overall dynamic state of the joint to be more strongly influenced by passive soft tissue and active quadriceps forces in terminal extension^{6,14,33}. The interaction between the contact, passive soft-tissue, and active quadriceps forces varies across subjects, further reducing the predictability of the dynamic state. For example, a large portion of the unexplained variance in SI_K may be attributed to its dependence on the nominal lengths and material properties of the patellar and quadriceps tendons, which can vary greatly across subjects, particularly in PFPS^{18,34}.

The static PTA was the only variable that strongly predicted its dynamic counterpart. This supports a previous study that found strong agreement between excessive lateral tilt measured using a clinical exam and measured using 2D static MRI.¹³ The strong relationship between the static PTA and PF dynamic lateral tilt may indicate that quadriceps activity has minimal effect on patellar tilt during terminal extension. Thus, even though the femoral sulcus influence diminishes in terminal extension, it may remain a controlling force for lateral patellar tilt⁴. The regression was likely further strengthened by the large range of

values for lateral tilt across both cohorts. Yet, this range in value is the likely reason why none of the recent 3D PF kinematics/alignment studies with active quadriceps reported significant differences in tilt between the PFPS and control cohorts¹⁸⁻²⁰.

In a previous study McWalter and colleagues³⁵ found that the value of a single measure of PF joint alignment, acquired statically at 30° flexion with active isometric quadriceps contraction, could not predict the slope (rate of change relative to knee angle) of 3D PF alignment measures acquired statically at various knee flexion angles in a cohort of healthy volunteers. This inability to predict the rate of change PF alignment may be due to the low reliability (0.58-0.59) in measuring slope using the static methodology reported by McWalter and colleagues²⁰. Although two previous studies^{18,20} have demonstrated significant differences in the slope of PF alignment/kinematic variables when comparing cohorts of subjects with PF pain to control cohorts, the clinical utility of evaluating slope has not been established. Thus, clinical diagnosis of maltracking remains focused on the value (not slope) of PF alignment/kinematics in terminal extension, as this is where the restraints of the femoral sulcus on the patella are weakest and pathology is typically most evident^{6,18,36}.

Several studies have investigated static joint alignment measures, yet few studies^{17,37-41} have reported the reliability of these measures. The reliability measures from the current study (0.94 – 0.99) were better than previous studies and satisfied the guideline for reasonable clinical validity (ICC>0.90)³⁸. Only one previous study evaluating patella alta^{37,40,41} reported “good” inter-rater reliabilities (ICC > 0.75³⁸). The studies measuring patellar tilt and BO reported good reliabilities for measures acquired during active leg extensions (ICC = 0.90¹⁷) and passively (ICC=0.76 for BO and ICC=0.86 for PTA)³⁹.

The primary limitation of this study was that specific static counterparts for dynamic PF flexion and varus rotation were not established, thus the predictability of these dynamic variables remained low. Another possible limitation was that the exercise evaluated was open-chain, whereas PF pain is most often thought to be exacerbated by weight-bearing (closed-chain) activities. Yet, PF pain can be induced during free extension¹⁹, as well as during long term stationary sitting with flexed knees⁴². Also, the exercise used in the current study emphasized the conditions of joint instability by requiring a quadriceps force in terminal extension, where the femoral constraints on the patella are at a minimum and pathomechanics are most evident. Based on the work of Hungeford⁴³, this required quadriceps force in terminal extension was likely greater than that required at or near full extension in previous studies evaluating PF kinematics during free squats^{19,44}. Regardless, this study clearly demonstrated the robustness of using specific static variables, such as the patellar tilt angle, to predict PF joint motion. Future studies should examine additional static surrogates for improved prediction.

In conclusion, static PF joint assessment cannot fully represent the dynamic state of this joint and using such static measures for diagnosis would likely produce false negative diagnoses^{7,15,17}. This makes it imperative that the current precise, accurate, 3D, dynamic imaging techniques be translated into clinical tools in order to improve the diagnosis of PF pathomechanics^{7,17,33,45} by providing accurate and precise quantification of PF kinematics,

which expands beyond the axial plane, during a volitional activity requiring quadriceps loading.

ACKNOWLEDGEMENTS

This research was supported by Biomedical Engineering Summer Internship Program (BESIP), the Intramural Research Program of the NIH, and the Clinical Center at the NIH. Special thanks is given to S. Sadeghi, AJ Behnam, C. Zampieri-Gallagher, TJ Brindle, CY Shieh, B. Damaska, and the Diagnostic Radiology Department at the NIH for their support and research time.

REFERENCES

1. Boling M, Padua D, Marshall S, et al. Gender differences in the incidence and prevalence of patellofemoral pain syndrome. *Scand J Med Sci Sports*. 2009
2. Amis AA. Current concepts on anatomy and biomechanics of patellar stability. *Sports Med Arthrosc*. 2007; 15:48–56. [PubMed: 17505317]
3. Keser S, Savranlar A, Bayar A, et al. Is there a relationship between anterior knee pain and femoral trochlear dysplasia? Assessment of lateral trochlear inclination by magnetic resonance imaging. *Knee Surg Sports Traumatol Arthrosc*. 2008; 16:911–915. [PubMed: 18553069]
4. Harbaugh CM, Wilson NA, Sheehan FT. Correlating femoral shape with patellar kinematics in patients with patellofemoral pain. *J Orthop Res*. 2010; 28:865–872. [PubMed: 20108348]
5. Sheehan FT, Derasari A, Fine KM, et al. Q-angle and J-sign: indicative of maltracking subgroups in patellofemoral pain. *Clin Orthop Relat Res*. 2010; 468:266–275. [PubMed: 19430854]
6. Brossmann J, Muhle C, Schroder C, et al. Patellar tracking patterns during active and passive knee extension: evaluation with motion-triggered cine MR imaging. *Radiology*. 1993; 187:205–212. [PubMed: 8451415]
7. Biedert RM, Sanchis-Alfonso V. Sources of anterior knee pain. *Clin Sports Med*. 2002; 21:335–347, vii. [PubMed: 12365231]
8. Farrokhi S, Keyak JH, Powers CM. Individuals with patellofemoral pain exhibit greater patellofemoral joint stress: a finite element analysis study. *Osteoarthritis Cartilage*. 2011; 19:287–294. [PubMed: 21172445]
9. Laurin CA, Levesque HP, Dussault R, et al. The abnormal lateral patellofemoral angle: a diagnostic roentgenographic sign of recurrent patellar subluxation. *J Bone Joint Surg Am*. 1978; 60:55–60. [PubMed: 624759]
10. Merchant AC, Mercer RL, Jacobsen RH, Cool CR. Roentgenographic analysis of patellofemoral congruence. *J Bone Joint Surg Am*. 1974; 56:1391–1396. [PubMed: 4433362]
11. Walker C, Cassar-Pullicino VN, Vaisha R, McCall IW. The patello-femoral joint--a critical appraisal of its geometric assessment utilizing conventional axial radiography and computed arthro-tomography. *Br J Radiol*. 1993; 66:755–761. [PubMed: 8220942]
12. Hunter DJ, Zhang YQ, Niu JB, et al. Patella malalignment, pain and patellofemoral progression: the Health ABC Study. *Osteoarthritis Cartilage*. 2007; 15:1120–1127. [PubMed: 17502158]
13. Grelsamer RP, Weinstein CH, Gould J, Dubey A. Patellar tilt: the physical examination correlates with MR imaging. *Knee*. 2008; 15:3–8. [PubMed: 18023186]
14. Sasaki T, Yagi T. Subluxation of the patella. Investigation by computerized tomography. *Int Orthop*. 1986; 10:115–120. [PubMed: 3744630]
15. Conway WF, Hayes CW, Loughran T, et al. Cross-sectional imaging of the patellofemoral joint and surrounding structures. *Radiographics*. 1991; 11:195–217. [PubMed: 2028059]
16. Stanford W, Phelan J, Kathol MH, et al. Patellofemoral joint motion: evaluation by ultrafast computed tomography. *Skeletal Radiol*. 1988; 17:487–492. [PubMed: 3201275]
17. Ward SR, Shellock FG, Terk MR, et al. Assessment of patellofemoral relationships using kinematic MRI: comparison between qualitative and quantitative methods. *J Magn Reson Imaging*. 2002; 16:69–74. [PubMed: 12112505]

18. Sheehan FT, Derasari A, Brindle TJ, Alter KE. Understanding patellofemoral pain with maltracking in the presence of joint laxity: complete 3D in vivo patellofemoral and tibiofemoral kinematics. *J Orthop Res.* 2009; 27:561–570. [PubMed: 19009601]
19. Wilson NA, Press JM, Koh JL, et al. In vivo noninvasive evaluation of abnormal patellar tracking during squatting in patients with patellofemoral pain. *J Bone Joint Surg Am.* 2009; 91:558–566. [PubMed: 19255215]
20. MacIntyre NJ, Hill NA, Fellows RA, et al. Patellofemoral joint kinematics in individuals with and without patellofemoral pain syndrome. *J Bone Joint Surg Am.* 2006; 88:2596–2605. [PubMed: 17142409]
21. Insall J, Goldberg V, Salvati E. Recurrent dislocation and the high-riding patella. *Clin Orthop Relat Res.* 1972; 88:67–69. [PubMed: 5086583]
22. Ali SA, Helmer R, Terk MR. Patella alta: lack of correlation between patellotrochlear cartilage congruence and commonly used patellar height ratios. *AJR Am J Roentgenol.* 2009; 193:1361–1366. [PubMed: 19843754]
23. Ward SR, Terk MR, Powers CM. Patella alta: association with patellofemoral alignment and changes in contact area during weight-bearing. *J Bone Joint Surg Am.* 2007; 89:1749–1755. [PubMed: 17671014]
24. Sheehan FT, Babushkina A, Alter KE. Kinematic determinants of anterior knee pain in cerebral palsy: a case-control study. *Arch Phys Med Rehabil.* 2012; 93:1431–1440. [PubMed: 22465585]
25. Shibanuma N, Sheehan FT, Stanhope SJ. Limb positioning is critical for defining patellofemoral alignment and femoral shape. *Clin Orthop Relat Res.* 2005:198–206. [PubMed: 15864053]
26. Powers CM, Bolgla LA, Callaghan M, et al. Patellofemoral pain: proximal, distal, and local factors, 2nd international research retreat. *J Orthop Sports Phys Ther.* 2012; 42:A1–A54. [PubMed: 22660660]
27. Behnam AJ, Herzka DA, Sheehan FT. Assessing the accuracy and precision of musculoskeletal motion tracking using cine-PC MRI on a 3.0T platform. *J Biomech.* 2011; 44:193–197. [PubMed: 20863502]
28. Seisler AR, Sheehan FT. Normative three-dimensional patellofemoral and tibiofemoral kinematics: a dynamic, in vivo study. *IEEE Trans Biomed Eng.* 2007; 54:1333–1341. [PubMed: 17605365]
29. Sheehan FT, Zajac FE, Drace JE. Using cine phase contrast magnetic resonance imaging to non-invasively study in vivo knee dynamics. *J Biomech.* 1998; 31:21–26. [PubMed: 9596534]
30. Sheehan FT, Mitiguy P. In regards to the “ISB recommendations for standardization in the reporting of kinematic data”. *J Biomech.* 1999; 32:1135–1136. [PubMed: 10476854]
31. Hebel, JR.; McCarter, RJ. A study guide to epidemiology and biostatistics. 7th ed.. Jones & Bartlett Learning; Sudbury, Mass: 2012. Correlations.; p. 90
32. Benjamini Y, Hochber Y. Controlling the False Discovery Rate: a Practical and Powerful Approach to Multiple Testing. 1995; 57:289–300.
33. Guzzanti V, Gigante A, Di Lazzaro A, Fabbriani C. Patellofemoral malalignment in adolescents. Computerized tomographic assessment with or without quadriceps contraction. *Am J Sports Med.* 1994; 22:55–60. [PubMed: 8129111]
34. Witvrouw E, Lysens R, Bellemans J, et al. Intrinsic risk factors for the development of anterior knee pain in an athletic population. A two-year prospective study. *Am J Sports Med.* 2000; 28:480–489. [PubMed: 10921638]
35. McWalter EJ, Macintyre NJ, Cibere J, Wilson DR. A single measure of patellar kinematics is an inadequate surrogate marker for patterns of three-dimensional kinematics in healthy knees. *Knee.* 2010; 17:135–140. [PubMed: 19720534]
36. Heegaard J, Leyvraz PF, Van Kampen A, et al. Influence of soft structures on patellar three-dimensional tracking. *Clin Orthop Relat Res.* 1994:235–243. [PubMed: 8119024]
37. Biedert RM, Albrecht S. The patellotrochlear index: a new index for assessing patellar height. *Knee Surg Sports Traumatol Arthrosc.* 2006; 14:707–712. [PubMed: 16496126]
38. Portney L, Watkins M. Statistical Measures of Reliability. *Foundations of Clinical Research Applications to Practice.* 2009

39. Jan MH, Lin DH, Lin CH, et al. The effects of quadriceps contraction on different patellofemoral alignment subtypes: an axial computed tomography study. *J Orthop Sports Phys Ther.* 2009; 39:264–269. [PubMed: 19346623]
40. Davies AP, Costa ML, Shepstone L, et al. The sulcus angle and malalignment of the extensor mechanism of the knee. *J Bone Joint Surg Br.* 2000; 82:1162–1166. [PubMed: 11132279]
41. Seil R, Muller B, Georg T, et al. Reliability and interobserver variability in radiological patellar height ratios. *Knee Surg Sports Traumatol Arthrosc.* 2000; 8:231–236. [PubMed: 10975264]
42. Kujala UM, Jaakkola LH, Koskinen SK, et al. Scoring of patellofemoral disorders. *Arthroscopy.* 1993; 9:159–163. [PubMed: 8461073]
43. Hungerford DS, Barry M. Biomechanics of the patellofemoral joint. *Clin Orthop Relat Res.* 1979; 144:9–15. [PubMed: 535256]
44. Powers CM, Ward SR, Fredericson M, et al. Patellofemoral kinematics during weight-bearing and non-weight-bearing knee extension in persons with lateral subluxation of the patella: a preliminary study. *J Orthop Sports Phys Ther.* 2003; 33:677–685. [PubMed: 14669963]
45. Schutzer SF, Ramsby GR, Fulkerson JP. Computed tomographic classification of patellofemoral pain patients. *Orthop Clin North Am.* 1986; 17:235–248. [PubMed: 3714207]

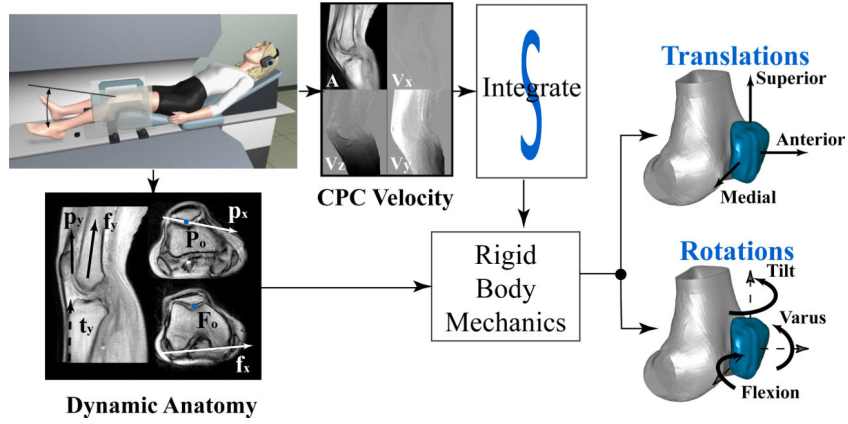


Figure 1. Flow chart for analysis of the dynamic data

The patellar and femoral medial directions (\mathbf{p}_x , \mathbf{f}_x) were parallel to the patellar lateral-posterior edge and the femoral posterior edge. In the mid-patellar sagittal image, the patellar posterior edge and the vector bisecting the distal femoral shaft defined the patellar and femoral superior direction ($\sim\mathbf{p}_y$, $\sim\mathbf{f}_y$). The 3D coordinate system was defined such that $\mathbf{p}_z = \mathbf{p}_x \times \sim\mathbf{p}_y$ and $\mathbf{p}_y = \mathbf{p}_z \times \mathbf{p}_x$. The knee angle was the acute angle between \mathbf{f}_y and \mathbf{t}_y (parallel to the tibial anterior edge, in a sagittal image just medial to the tibial tuberosity). The static coordinate system and knee angle used identical definitions. **Abbreviations:** A: anatomic image; V_x , V_y , and V_z : velocity in the x, y, and z directions, respectively; CPC: Cine Phase Contrast; P_o and F_o : Origin of the patellar and femoral coordinate systems, respectively.

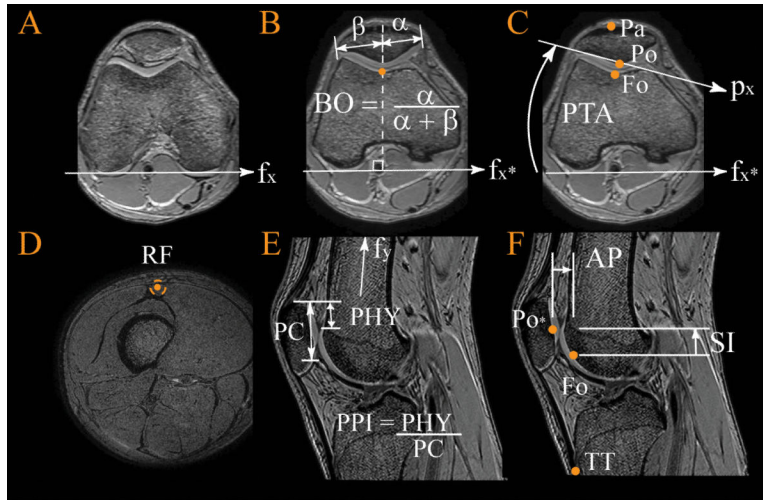


Figure 2. Static Magnetic Resonance Imaging-based Measures of Patellofemoral Alignment

A) f_x = the femoral medial direction, which was defined by the most posterior points on the medial and lateral condyles at the level of the epicondylar width. B) BO = bisect offset; f_x^* a representation of the femoral medial axis as defined in A; α and β = the shortest distance from the most medial and lateral patellar points, respectively, to a line perpendicular to f_x that passes through F_o , propagated to the mid-patellar plane. C) PTA = patellar tilt angle; P_o and F_o = origin of the patellar and femoral coordinate systems; p_x = the patellar medial direction; P_a = anterior patella. D) RF = rectus femoris. E) PPI = patellophyseal index; PC = length of patellar articular cartilage; PHY = height of patella above anterior physeal line. F) AP = anterior/posterior distance; SI = superior/inferior distance; P_o^* - a representation of P_o , which is defined in C; TT= tibial tuberosity.

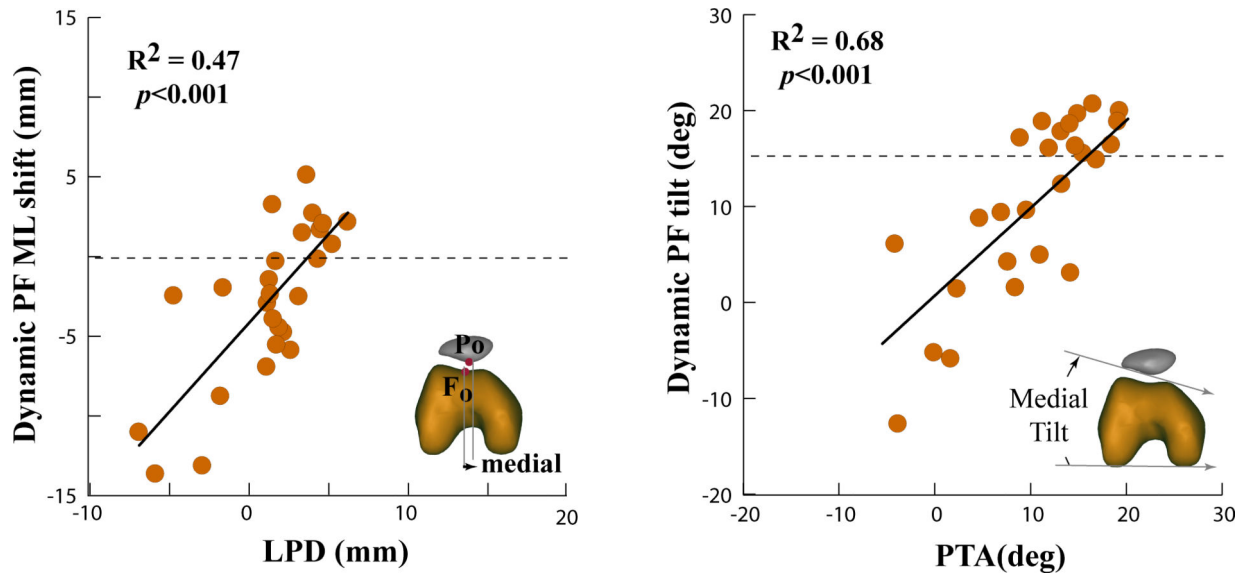


Figure 3. Example Linear Regression Plots for the Patellofemoral Pain Syndrome Cohort
 Control averages for the dynamic variables are provided with a dotted line. **Abbreviations:**
 PTA: patellar tilt angle; ML= the medial-lateral location of the patellar origin relative to the femoral origin; LPD= lateral patellar displacement; deg= degree; mm= millimeter; r^2 = coefficients of determination.

Table 1

Intraclass Correlation Coefficients for static Magnetic Resonance Imaging-based Surrogates.

Parameter	PTA	BO	LPD	SI _s	AP _s	RF Q-angle
Inter	0.995	0.985	0.979	0.990	0.948	0.985
Intra	0.993	0.980	0.968	0.992	0.953	0.989

Abbreviations: PTA= patellar tilt angle; BO= Bisect Offset; LPD, AP_s and SI_s= The medial-lateral, anterior-posterior, and superior-inferior location of the patellar origin relative to the femoral origin (static); RF-Q angle= The rectus femoris quadriceps angle.

Author Manuscript

Author Manuscript

Author Manuscript

Author Manuscript

Table 2

Coefficients of determination (r^2) for the control (C), patellofemoral pain syndrome (PFPS), and combined (All) cohorts

	All	C	PFPS	All	C	PFPS	All	C	PFPS
Translations	ML_K			SI_K			AP_K		
BO	0.27 **		0.32						
LPD	0.32 **		0.47 **	0.22 **		0.43 **			
AP_S							0.18		
SI_S				0.43 **	0.48 **	0.38 **			
PPI				0.28 **	0.36 **	0.26 **			
PTA	0.23 **		0.31						
RF-Q	0.19		0.35			0.30			
Rotations	Flexion			Tilt			Varus		
BO				0.49 **	0.27	0.54 **			
LPD				0.23 **		0.29			
AP_S									
SI_S	0.26 **	0.42 **							
PPI	0.23 **	0.41 **							
PTA				0.69 **	0.59 **	0.68 **	0.17		
RF-Q				0.16		0.37			

Nonsignificant regressions are not shown. For the full regression equations, see supplemental material.

Abbreviations: BO = Bisect Offset; LPD, AP_S, and SI_S = The static medial-lateral, anterior-posterior, and superior-inferior location of the patellar origin relative to the femoral origin (static); PPI = patellophyseal index; PTA = patellar tilt angle; RF-Q angle = The rectus femoris quadriceps angle; ML_K, SI_K, AP_K = The medial-lateral, superior-inferior, and anterior posterior location of the patellar origin relative to the femoral origin, measured during active extension at 10° knee angle.

** Indicates $p < 0.001$, otherwise $p < 0.05$.

Table 3

Multiple Regression Equations.

Dynamic Variable	Multiple Regressions	R ²	p- value
All			
ML_K	= -4.61 + 0.61*LPD -0.15*PTA	0.38	<0.001
SI_K	= 13.48 -0.62*SI _S -0.38*LPD-0.14*RF_Q	0.53	<0.001
Flexion	= 8.435 -0.40*SI _S -0.57*PA _S	0.36	<0.001
PFPS Cohort			
ML_K	= -4.14 + 1.52*LPD -0.13*RF_Q	0.62	<0.000
AP_K	= 2.34 -0.50*AP _S -0.001*RF_Q	0.38	0.001
SI_K	= 16.80 + 0.51*SI _S -1.45*LPD +0.15*RF_Q	0.77	<0.001
Flexion	= 7.553 -0.307*SI _S -0.540*AP _S	0.32	0.003
Control Cohort			
Flexion	= 20.816 -0.514*SI _S -0.383*PTA	0.65	<0.001

Multiple Regressions listed if it increased the predictability more than 5 percentage points from the linear regression.

Abbreviations: ML_K, SI_K, AP_K = The medial-lateral, superior-inferior, and anterior-posterior location of the patellar origin relative to the femoral origin measured during active extension at 10° knee angle; LPD, AP_S, and SI_S = the static medial-lateral, anterior-posterior, and superior-inferior location of the patellar origin relative to the femoral origin; PTA = patellar tilt angle; RF-Q angle = The rectus femoris quadriceps angle.